Modeling Atherosclerotic Plaque Growth: A Case Report Based on a 3D Geometry of Left Coronary Arterial Tree from Computed Tomography

Antonis I. Sakellarios, Panagiotis K. Siogkas, Lambros S. Athanasiou, Themis P. Exarchos, Member, IEEE, Michail I. Papafaklis, Christos V. Bourantas, Katerina K. Naka, Dimitra Iliopoulou, Lampros K. Michalis, Nenad Filipovic, Oberdan Parodi and Dimitrios I. Fotiadis, Senior Member, IEEE

***Abstract*—In this study, we present an innovative model for plaque growth utilizing a 3-Dimensional (3D) left coronary arterial tree reconstructed from computed tomographic (CT) data. The proposed model takes into consideration not only the effect of the local hemodynamic factors but also major biological processes such as the low density lipoprotein (LDL) and high density lipoprotein (HDL) transport, the macrophages recruitment and the foam cells formation. The endothelial membrane is considered semi-permeable and endothelial shear stress dependent, while its permeability is modeled using the Kedem-Katscalsky equations. Patient specific biological data are used for the accurate modeling of plaque formation process. The finite element method (FEM) is employed for the solution of the system of partial differential equations. The results of the simulation are compared to the plaque progression in a follow-up CT examination performed three years after the initial investigation. The results show that the proposed model can be used to predict regions prone for plaque development of progression.**

I. Introduction

CARDIOVASCULAR disease is one of the most common causes of death in west societies [1]. Atherosclerosis is characterized by the thickening and obstruction of the arterial lumen and is considered as a multi-factorial process, which is affected by the local hemodynamic, biological and genetic factors. Evidence from clinical studies have shown that the endothelial shear stress (ESS) infuence plaque initiation and formation with the regions being explosed to low ESS or disturbed flow recirculation to be prone for plaque formation [2]. Dislipidemia (i.e., increased LDL or low HDL concentration) has been also associated with an increased risk for plaque development. Finally, many genetic disorders affect the atherosclerotic process through several pathophysiological pathways which determine endothelial permeability foam cells formation and macrophages accumulation.

The recent years, finite element methods have been widely used for modeling biological processes such as atherosclerosis. The first studies were based on modeling blood flow and the effect of the ESS on plaque formation and compositional characteristics [3,4].

Besides blood flow modeling, several computational studies have been presented modeling other processes of atherosclerosis. Most of these studies focused on LDL transport and implemented several different modeling approaches. Some assumed that the endothelium is non-permeable [5,6], others that the arterial wall as a simple homogenous layer or multilayer; few that the endothelial permeability is shear dependent [7-9], while others attempted to include mitosis and apoptosis processes that alter the endothelial permeability [10,11].

In this work, we present a novel mathematical model for plaque growth. In this approach, we take into account the major processes that are involved in plaque growth including: i) the local hemodynamics, ii) LDL and HDL transport, iii) LDL oxidation, iv) inflammation and macrophages migration and, v) foam cells formation based on oxidized LDL and macrophages concentration. We use realistic patient's data(CT images) to reconstruct coronary geometry at baseline and compare our computational findings with the changes in plaque distribution at a follow up examination performed three years later.

This work was supported by the EU project ARTreat FP7-224297, Multi-level patient-specific artery and atherogenesis model for outcome prediction, decision support treatment, and virtual hand-on training.

A.I. Sakellarios, L.S. Athanasiou, P.K. Siogkas and D.I. Fotiadis are with the Unit of Medical Technology and Intelligent Information Systems, Dept. of Materials Science and Engineering, University of Ioannina, GR 45110 (email: ansakel@cc.uoi.gr, lmathanas@cc.uoi.gr, psiogkas@cc.uoi.gr corresponding author phone: +302651008803; fax: +302651008889; e-mail: fotiadis@cs.uoi.gr).

T.P. Exarchos is with the Institute of Molecular Biology and Biotechnology, Dept. of Biomedical Research, FORTH, GR45110, Ioannina, Greece (email: exarchos@cc.uoi.gr)

M.I Papafaklis is with the Cardiovascular Division, Brigham and Women's Hospital, Harvard Medical School, Boston, USA (email: m.papafaklis@yahoo.com)

C.V. Bourantas is with the Dept. of Interventional Cardiology, Erasmus MC, Thoraxcenter, Rotterdam, The Netherlands (email: cbourantas@gmail.com)

K.K. Naka and L.K. Michalis are with the Michaelideion Cardiac Center, Dept. of Cardiology in Medical School, University of Ioannina, GR 45110 Ioannina, Greece (email: anaka@cc.uoi.gr, lmihalis@cc.uoi.gr).

D. Iliopoulou is with the institute of communication and computer systems

N. Filipovic is with the University of Kragujevac, Serbia (e-mail: fica@kg.ac.rs)

O. Parodi is with the Institute of Clinical Physiology, National Research Council, 56124, Pisa, Italy (email: oberpar@tin.it).

978-1-4799-3163-7/13/$31.00 ©2013 IEEE

II. Materials and Methods

A. Patient's data

A female patient with multiple risk factors (hypertension, diabetes, hypercholesterolemia and a family history of coronary artery disease) with an atypical chest pain underwent coronary CT in 2009. This examination showed atherosclerotic plaque on right and left anterior descending coronary artery (RCA; LAD), but without significant stenosis. She was put on medical standard of care treatment and did not have any further investigations. Three years later the she was re-admitted with an episode of epigastric pain and had a follow-up CT angiography that showed plaque progression in the mid LAD (percentage diameter stenosis 18% at baseline vs 53% at follow-up, Fig. 1).

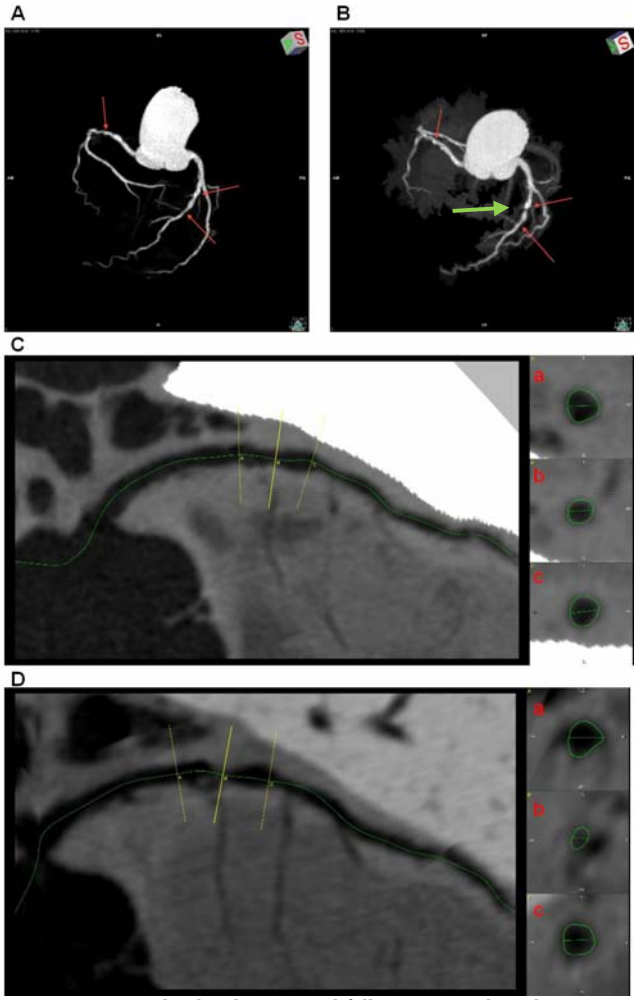

Fig 1. CT acquired at baseline (A) and follow-up (B). The red arrows in the 3d maximum intensity projection (MIP) reconstructions indicates 3 non-obnstructive plaques while the green arrow an now lesion detected at 3 years follow-up. (C, D) Multi-planar reconstruction (MPR) of the LAD at baseline and follow up, respectively. The reference planes of the axial slices shown at the right panels (a, b, c) are indicated in yellow in the main left panel. Slice b shows the site of the progressed lesion.

B. 3D reconstruction

Sato's Vesselness Filter was applied to improve image quality and contrast between different objects in the CT slices, while the Frangi Vesselness Filter [12] was used in each slice to enhance objects similar to vessels and exclude large objects like aorta. The borders of the vessel were roughly extracted using the Sobel edge detection algorithm and the obtained 2D binary slices were sequentially grouped, resulting in a 3D binary set of images. Then, 26-connected pixels neighbor connectivity was used to mark the voxels that belong to the selected artery. The algorithm produced single branches, detecting possible bifurcations. The above procedure was applied to each branch.

From the voxels belonging to a single branch, the centerline (3D path) was extracted by computing the center of gravity of each rough artery border [13]. The initial centerline is smoothed, downsampled and fitted using b-splines for the calculation of the gradient vector on each centerline point. The gradient is used to extract a perpendicular radius image (PRI) at each point which is used to detect the lumen and outer vessel wall border. From each RPI image we extracted the Region of Interest (ROI) of the artery by detecting the zero crosses and removing the area below the zero cross. Finally, the classification is based on a 3-component Gaussian Mixture Model (GMM) [14]. The 3D reconstructed geometries of the arterial tree are shown in Fig. 2.

Figure 2. 3D reconstructed left coronary arterial tree (red color: lumen; transparent grey color: outer wall).

C. Modeling blood flow

Blood flow in the arterial lumen was modeled using the Navier-Stokes equations and the continuity equation:

$$-\mu\nabla^2\mathbf{u}_l + \rho(\mathbf{u}_l\cdot\nabla)\mathbf{u}_l + \nabla p_l = 0\,, \qquad (1)$$

$$\nabla\cdot\mathbf{u}_l = 0\,, \qquad (2)$$

where l refers to the lumen, $\mathbf{u}_l$ is the blood velocity, p_l is the pressure, μ is the dynamic viscosity of blood, and ρ is the blood density.

Plasma filtration in the arterial wall was modeled using Darcy's Law:

$$u_w - \nabla \cdot \left(\frac{\kappa_w}{\mu_p} p_w \right) = 0 , \quad (3)$$

where p_w is the pressure in the arterial wall and u_w is the plasma velocity and k_w is the Darcian permeability.

D. Modeling plaque growth

Plaque growth is modeled considering the main pathophysiological processes which occur during atherosclerotic plaque development: i) LDL and HDL transport, ii) LDL oxidation, iii) macrophage recruitment and iv) foam cell formation.

We modeled LDL and HDL transport in the arterial lumen using the convection-diffusion equations:

$$\nabla \cdot \left(-D_{l,LDL} \nabla c_{l,LDL} + c_l u_{l,LDL} \right) = 0 , \quad (4)$$

$$\nabla \cdot \left(-D_{l,HDL} \nabla c_{l,HDL} + c_l u_{l,HDL} \right) = 0 , \quad (5)$$

where l indicates the lumen domain, LDL and HDL the molecules which are transported, D is the diffusivity in the lumen and c is the molecule concentration. Additionally, we model LDL transport in the arterial wall using a convection-diffusion-reaction equation:

$$\nabla \cdot \left(-D_{w,LDL} \nabla c_{w,LDL} + k c_{w,LDL} u_{w,LDL} \right) = r_{w,LDL} c_{w,LDL} , \quad (6)$$

where D_w is the diffusivity in the wall, r_w is the consumption rate constant and k is the solute lag coefficient.

LDL oxidation was modeled taking into account the athero-protective role of HDL. Data presented in [15] were used for this purpose. Necessary fitting of the experimental data was made in order to represent physiological human values. Details about the LDL oxidation and the fitting of the experimental data can be found in [16]. The oxidation of LDL was modeled using a diffusion-reaction equation:

$$d \Delta O + O \cdot M + r_{w,LDL} c_{w,LDL} + HDL_{\ protection} = 0 , \quad (7)$$

where O is the oxidized LDL, d is the diffusion coefficient and M is the number of white blood cells. The equation requires as inlet boundary condition the calculated LDL concentration, while the reaction term of the equation takes into account the HDL concentration. $HDL_{protection}$ was defined by the experimentally observed relation shown in Fig. 3.

Finally, macrophage migration and foam cell formation are modeled using the following equations:

$$\partial_t M + div(v_w M) = d_2 \Delta M - k_1 Ox \cdot M + S/(1+S) , \quad (8)$$

$$\partial_t S = d_3 \Delta S - \lambda S + k_1 Ox \cdot M + \gamma (Ox - O_x^{thr}) , \quad (9)$$

$$\nabla v_w = k_1 Ox \cdot M , \quad (10)$$

where d_2 and d_3 are diffusion coefficients for macrophages and cytokines, respectively. S is the cytokines concentration, k_1 is the growing plaque coefficient, and λ and γ are the degradation coefficients for the cytokines and the oxidized LDL, respectively.

The boundary conditions applied for mass transport were a constant concentration for LDL ($C_{0,LDL}$) and HDL ($C_{0,HDL}$) at the inlet and the adventitia boundary ($0.005C_0$) and a convective flow at the outlet of the artery.

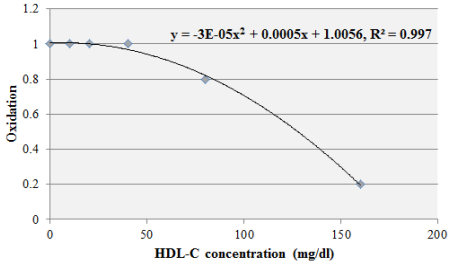

Figure 3. Relation of LDL oxidation rate with HDL concentration. The fitting and the extraction of the relation is described in [16].

Kedem-Katchalsky equations were used to model the interaction between the lumen and the arterial wall at the endothelial membrane layer:

$$J_v = L_p \left(\Delta p - \sigma_d \Delta \pi \right) , \quad (11)$$

$$J_s = P \Delta c + \left(1 - \sigma_f \right) J_v \bar{c} , \quad (12)$$

where L_p is the hydraulic conductivity of the endothelium; Δc is the solute concentration difference, Δp is the pressure drop and $\Delta \pi$ is the oncotic pressure difference, in the endothelium; σ_d is the osmotic reflection coefficient, σ_f is the solvent reflection coefficient, P is the solute diffusive endothelial permeability, and c is the concentration. We assumed that hydraulic conductivity depends on ESS according to the study of Sun et al. [7]. Finally, we assumed that at the adventitia boundary macrophages and cytokines concentration are zero, while at the endothelial boundary the macrophages migration is given as:

$$\partial M = \frac{k_1 S}{1 + k_2 S} . \quad (13)$$

III. Results – Discussion

Simulation was performed at the left coronary arterial tree of the patient that was reconstructed from the baseline CT data. About two millions hexahedral elements and three millions bridges elements were used for the lumen and outer wall domain, respectively.

Fig. 4 shows the ESS distribution and the regions of low ESS, where it is clear that low ESS regions are found at the bifurcations where flow disturbances are often noted. The average ESS was 2.7Pa, while about 35% of the total endothelial surface presented athero-promoted (<1 Pa) low ESS values (Fig. 4(B).

In Fig. 5(A), the calculated LDL concentration is shown. LDL concentration is increased in low ESS regions due to the concentration polarization at the luminal endothelial side. Oxidized LDL is depicted in Fig. 5(B). It is apparent that there is a difference between the distribution of the oxidized LDL and the LDL concentration. This is due to the

protective effect of HDL to the LDL oxidation.

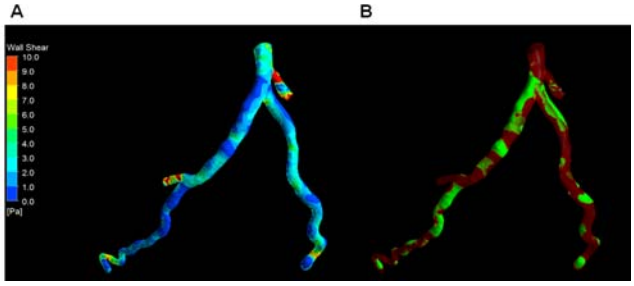

Figure 4. (A) ESS distribution, (B) regions of low ESS (0-1Pa) indicated with a green color. Low ESS is especially observed at the bifurcations.

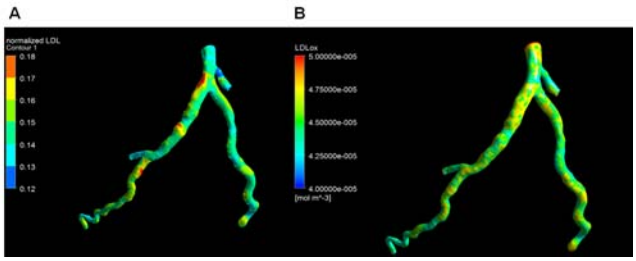

Figure 5. (A) Distribution of LDL concentration. (B) Concentration of oxidized LDL.

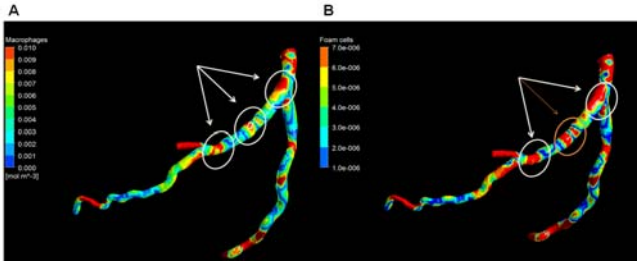

Figure 6. Macrophages (A) and foam cells (B) concentration. Circles show the plaque regions.

Finally, Fig. 6 shows the calculated macrophages and foam cells concentration. Comparing the macrophages concentration with the follow up examination (Fig 1(B)) it is clear that increased concentrations are observed at the regions with plaque. Moreover, the accumulation of foam cells is more obvious than macrophages, especially regarding the progressed lesion (orange arrow). A limitation is that the model may depict and other potential plaque regions.

IV. Conclusion

In the current work, we modeled atherosclerotic plaque growth in a left coronary arterial tree reconstructed using CT data. The proposed model includes many pathophysiological pathways involved in plaque growth: LDL / HDL transport, LDL oxidation, macrophage migration and foam cell formation. Thus, it is likely this model to provide more accurate identification of vulnerable segments and may have a value in the prediction of future culprit lesions.

References

[1] World Health Organization. Cardiovascular Diseases, 2009.

[2] P. Stone, S. Saito, S. Takahashi, Makita Y, *et al*., "Prediction of progression of coronary artery disease and clinical outcomes using vascular profiling of endothelial shear stress and arterial plaque characteristics: the PREDICTION Study," Circulation. Vol. 126(2), pp. 172-81, 2012.

[3] H. Samady, P. Eshtehardi, M. McDaniel, J. Suo, S. Dhawan, C. Maynard, L. Timmins, A. Quyyumi, D. Giddens. "Coronary artery wall shear stress is associated with progression and transformation of atherosclerotic plaque and arterial remodeling in patients with coronary artery disease," Circulation, Vol. 124(7), pp. 779-88, 2011.

[4] P. Stone, S. Saito, S. Takahashi, Y. Makita, S. Nakamura, T. Kawasaki, A. Takahashi, *et al*. "Prediction of Progression of Coronary Artery Disease and Clinical Outcomes Using Vascular Profiling of Endothelial Shear Stress and Arterial Plaque Characteristics: The PREDICTION Study," Circulation, Vol. 126(2), pp. 172-181, 2012.

[5] M. Kaazempur-Mofrad, C. Ethier. "Mass transport in an anatomically realistic human right coronary artery," Ann Biomed Eng, Vol. 29, pp. 121–127, 2001.

[6] M. Kaazempur-Mofrad, S. Wada, J. Myers, C. Ethier. "Mass transport and fluid flow in stenotic arteries: axisymmetric and asymmetric models," Int J Heat Mass Transfer, Vol. 48, pp. 4510–4517, 2005.

[7] N. Sun, R. Torii, N. Wood, A. Hughes, S. Thom, X. Xu. "Computational modeling of LDL and albumin transport in an in vivo CT image based human right coronary artery," J Biomech Eng, Vol. 131, pp. 021003–021003, 2009.

[8] N. Filipovic, et al., "ARTreat Project: Three-Dimensional Numerical Simulation of Plaque Formation and Development in the Arteries," IEEE Transactions on Information Technology in Biomedicine, Vol. 16, pp. 272-278, Mar 2012.

[9] O. Parodi, et al., "Patient-Specific Prediction of Coronary Plaque Growth From CTA Angiography: A Multiscale Model for Plaque Formation and Progression," Ieee Transactions on Information Technology in Biomedicine, Vol. 16, pp. 952-965, Sep 2012.

[10] U. Olgac, V. Kurtcuoglu, and D. Poulikakos, "Computational modeling of coupled blood-wall mass transport of LDL: effects of local wall shear stress," American Journal of Physiology-Heart and Circulatory Physiology, Vol. 294, pp. H909-H919, Feb 2008.

[11] U. Olgac, D. Poulikakos, S. C. Saur, H. Alkadhi, and V. Kurtcuoglu, "Patient-specific three-dimensional simulation of LDL accumulation in a human left coronary artery in its healthy and atherosclerotic states," American Journal of Physiology-Heart and Circulatory Physiology, Vol. 296, pp. H1969-H1982, Jun 2009.

[12] R. F. Frangi, W. J. Niessen, K. L. Vincken, and M. A. Viergever, "Multiscale vessel enhancement filtering," in Lecture Notes in Computer Science, ed: Springer-Verlag, 1988, pp. 130-137.

[13] H. Kokubun, O. Miyazaki, and H. Hayashi, "Radial intensity projection for lumen: application to CT angiographic imaging," presented at the Medical Imaging 2006: Physics of Medical Imaging, San Diego, 2006.

[14] O. Klass, S. Kleinhans, M. J. Walker, M. Olszewski, S. Feuerlein, M. Juchems, and M. H. Hoffmann, "Coronary plaque imaging with 256-slice multidetector computed tomography: interobserver variability of volumetric lesion parameters with semiautomatic plaque analysis software," Int J Cardiovasc Imaging, Vol. 26, pp. 711-20, Aug 2010.

[15] S. T. Kunitake, M. R. Jarvis, R. L. Hamilton, and J. P. Kane, "Binding of Transition-Metals by Apolipoprotein-a-I-Containing Plasma-Lipoproteins - Inhibition of Oxidation of Low-Density Lipoproteins," Proceedings of the National Academy of Sciences of the United States of America, Vol. 89, pp. 6993-6997, Aug 1 1992.

[16] A. Sakellarios, P. Siogkas, L. Athanasiou, T. Exarchos, M. Papafaklis, C. Bourantas, K. Naka, L. Michalis, N. Filipovic, O. Parodi, D. Fotiadis, "Three-dimensional modeling of oxidized-LDL accumulation and HDL mass transport in a coronary artery: A proof-of-concept study for predicting the region of atherosclerotic plaque development", Proceedings of the Annual International Conference of the IEEE Engineering in Medicine and Biology Society, EMBS,2013, Osaka.

[17] A. Sakellarios, M. Papafaklis, P. Siogkas, L. Athanasiou, T. Exarchos, K.. Stefanou, C. Bourantas, K. Naka, L. Michalis, O. Parodi, D. Fotiadis, "Patient-specific computational modeling of subendothelial LDL accumulation in a stenosed right coronary artery: Effect of hemodynamic and biological factors," American Journal of Physiology – Heart and Circulatory Physiology. Vol. 304(11), pp. H1455-H1470, 2013, 2013.